Marine Heatwaves on the Northeast US continental shelf

Bachelor Thesis

B. Sc. Physics of the Earth System:
Meteorology, Oceanography, Geophysics

Christian-Albrechts-Universität Kiel
GEOMAR Helmholtz Center for Ocean Research
Woods Hole Oceanographic Institution

Author: Hendrik Großelindemann

Matriculation Number: 1123082

First Examiner: Prof. Dr. Arne Biastoch

Second Examiner: Dr. Svenja Ryan

December 2020

I. Abstract

Marine Heatwaves (MHWs) are climate events characterized by anomalously high temperatures that can have devastating impacts on ecosystems and therefore also on fisheries. MHWs increase in duration, frequency and intensity globally. Due to the lack of subsurface observations, the current knowledge about MHWs is mainly based on the surface, although MHWs have known impacts on pelagic and benthic ecosystems as well. This study investigates the depth structures of MHWs on the northeast US continental shelf with an ocean circulation model of 1/20° resolution. The Northwest Atlantic is one of the most rapidly warming regions in the world and as a consequence acutely exposed to MHWs. The shelf region especially is highly biologically productive resulting in a large fishing industry. Enormous impacts of MHWs have already been experienced in the recent decade. This study highlights a significant increase of MHWs duration and intensity on the shelf during the last 40 years, based on observed satellite SST data. It then briefly validates the effect of model resolution in resolving the prevailing ocean dynamics in this region that may be relevant for the generation of MHWs. It is shown that MHWs occur in various spatial extents. Some events appear only at the surface and are focused on the coastal region, whereas other events appear at depth at the shelf break, without reaching the surface. In addition, events occur which affect the whole water column. The highest temperature anomalies can be found at depth at the shelf break. Furthermore, associated salinity anomalies show similar patterns to temperature in deep events, whereas surface events show no connection of salinity and temperature. These discrepancies indicate different MHW drivers. Surface events can be likely linked to atmosphere ocean interactions. Deep events reveal Gulf Stream warm core ring interaction, where the eddy is able to intrude its anonymously warm and salty waters on to the shelf. Hence, MHW formation depends on the local dynamics whose better understanding is therefore necessary. This study shows the possible impacts of deep events and thus underlines the need of continuous subsurface measurements to detect MHWs at depth. Furthermore, this study reveals the opportunities of climate models to investigate MHWs, their characterization and associated drivers.

II. Zusammenfassung

Marine Hitzewellen (MHWs) sind Klimaereignisse, die durch außergewöhnlich hohe Temperaturen gekennzeichnet sind und verheerende Auswirkungen auf Ökosysteme und damit auf die Fischerei haben können. MHWs nehmen global an Dauer, Häufigkeit und Intensität zu. Aufgrund des Mangels an Beobachtungen in der Tiefe konzentriert sich das derzeitige Wissen über MHWs hauptsächlich auf die Oberfläche, auch wenn MHWs bekanntermaßen Auswirkungen auf pelagische und benthische Ökosysteme haben. Diese Studie untersucht die Tiefenstrukturen von MHWs auf dem nordöstlichen US-Kontinentalschelf mit Hilfe eines Modells mit 1/20° Auflösung. Der Nordwestatlantik ist eine der sich am schnellsten erwärmenden Regionen der Welt und als Folge davon akut MHWs ausgesetzt. Besonders die Schelfregion ist biologisch hochproduktiv, was zu einer großen Fischereiwirtschaft führt. In den letzten zehn Jahren traten bereits MHWs mit enormen Auswirkungen auf. Diese Studie zeigt eine signifikante Zunahme der Dauer und Intensität der MHWs auf dem Schelf während der letzten 40 Jahre, basierend auf Oberflächentemperaturen durch Satellitenmessungen. Der Effekt von Modellauflösung zur Reproduktion der vorherrschenden Dynamik in dieser Region wird kurz gezeigt. Dieses Modell wird dann verwendet, um die Tiefenstruktur von MHWs zu bestimmen. Es kann gezeigt werden, dass MHWs in verschiedenen räumlichen Ausdehnungen auftreten. Einige Ereignisse treten nur an der Oberfläche auf und konzentrieren sich auf die Küstenregion, während andere Ereignisse in der Tiefe auf den shelf break (Übergang vom Kontinetalschelf zum -hang) fokussiert sind, ohne die Oberfläche zu erreichen. Darüber hinaus treten Ereignisse auf, die die gesamte Wassersäule betreffen. Die höchsten Temperaturanomalien werden in der Tiefe am shelf break gefunden. Außerdem zeigen assoziierte Salzgehaltsanomalien ähnliche Muster wie die Temperatur bei Ereignissen in der Tiefe, während Ereignisse an der Oberfläche keinen Zusammenhang zwischen Salzgehalt und Temperatur aufweisen. Diese Diskrepanzen lassen auf unterschiedliche MHW-Treiber schließen. Oberflächenereignisse können mit Wechselwirkungen zwischen Atmosphäre und Ozean in Verbindung gebracht werden. Ereignisse in der Tiefe zeigen Einflüsse von Wirbeln, welche warmes und salziges Golfstrom Wasser auf den Schelf transportieren können. Daher hängt die MHW-Bildung von der lokalen Ozeandynamik ab, deren besseres Verständnis notwendig ist. Diese Studie zeigt die möglichen Auswirkungen von MHWs in der Tiefe und unterstreicht damit die Notwendigkeit kontinuierlicher Tiefenmessungen, um MHWs in der Tiefe nachzuweisen. Außerdem zeigt diese Studie die Möglichkeiten, die Klimamodelle zur Untersuchung von MHWs, ihrer Charakterisierung und der damit verbundenen Treiber, bieten können.

III. Table of Contents

I Abstract **I**

II Zusammenfassung **II**

III Table of Contents **III**

1 Introduction **1**

2 Data **4**
2.1 OISST 4
2.2 Sea Surface Height 4
2.3 Oleander Line 4
2.4 ORCA025 5
2.5 VIKING20X 5

3 Methods **6**
3.1 Marine Heatwave Detection 6
3.2 Model Validation 7
3.3 MHWs in VIKING20X 7

4 Results **9**
4.1 Characteristics and trends of MHWs 9
4.2 Modelled vs. observed regional hydrography 10
4.3 VIKING20X Climatology 12
4.4 MHWs on the shelf 13
4.5 Depth structure and associated drivers 15

5 Discussion **21**

6 References **25**

7 Appendix **29**

1. Introduction

Marine Heatwaves (MHWs) are extreme events described as discrete, prolonged and anomalously warm (*Hobday et al.*, 2016). They can have enormous impacts on marine ecosystems and therefore on socioeconomics, by causing mass mortality (*Mills et al.*, 2013; *Short et al.*, 2015; *Jones et al.*, 2018) or species redistribution (*Wernberg*, 2020; *Smale et al.*, 2019) which can influence fisheries and local economics (*Mills et al.*, 2013). These impacts might increase due to global warming. *Frölicher and Laufkötter* (2018) and *Oliver et al.* (2018, 2020) show an increase of MHW frequency, duration and intensity. These trends underline the need of improvement in the understanding of MHWs, their physical properties and possible impacts.

The northwest Atlantic and the northeast US continental shelf as a part of it are among the fastest warming regions in the world (*Wu et al.*, 2012; *Saba et al.*, 2015; *Forsyth et al.*, 2015). This exposes the region to a risk of increased occurrence and possible effects of MHWs. The recent decade has already experienced MHWs with drastic impacts even leading to international tensions (*Mills et al.*, 2013; *Gawarkiewicz et al.*, 2019). In addition to the changing thermodynamics, climate change has an influence on the local current system, which is highly complex in the first place. The warm and salty Gulf Stream flows poleward being the western boundary current of the North Atlantic subtropical gyre Figure 1. After separating at Cape Hatteras, the current starts to meander, which leads to eddy emergence. Generated Warm Core Rings (WCRs), which are anticyclonic mesoscale eddies, then propagate westward in the direction of the US coast and its shelf seas, advecting warm and salty waters in to this region (*Fratantoni and Pickart*, 2007). These WCRs can interact with shelf waters or even intrude their properties on to the shelf (*Gawarkiewicz et al.*, 2018). *Gangopadhyay et al.* (2019) found a significant regime shift in WCR occurrence around 2000, leading to additional WCRs per year. *Andres* (2016) showed a recent trend indicating a westward movement of the Gulf Stream destabilization point. This denotes that the Gulf Stream starts meandering further west which leads to increased open-ocean/shelf interaction.

The Shelf Break Jet is a cold and fresher current flowing equatorward from the Labrador Sea until Cape Hatteras right at the surface above the shelf break (*Forsyth et al.*, 2020). The Shelf Break Front describes the transition from cold and fresh shelf waters to warm and salty offshore waters (*Gawarkiewicz et al.*, 2018). The Shelf Break Jet and the slope front can act as a dynamical barrier for offshore water to intrude onto the continental shelf. Another dynamical aspect in this region is the recirculation gyre (*Csanady and Hamilton*, 1988). It is a cyclonic gyre between the Gulf Stream and the Shelf Break Jet in the most western part of slope sea (Figure 1, slope boxes A,B). Gulf Stream waters

recirculate into the shelf region at the eastern part while shelf waters enter the Gulf Stream at the western end of the gyre. All these dynamics interact with each other and a lot of research is currently done to increase the understanding of this complex system.

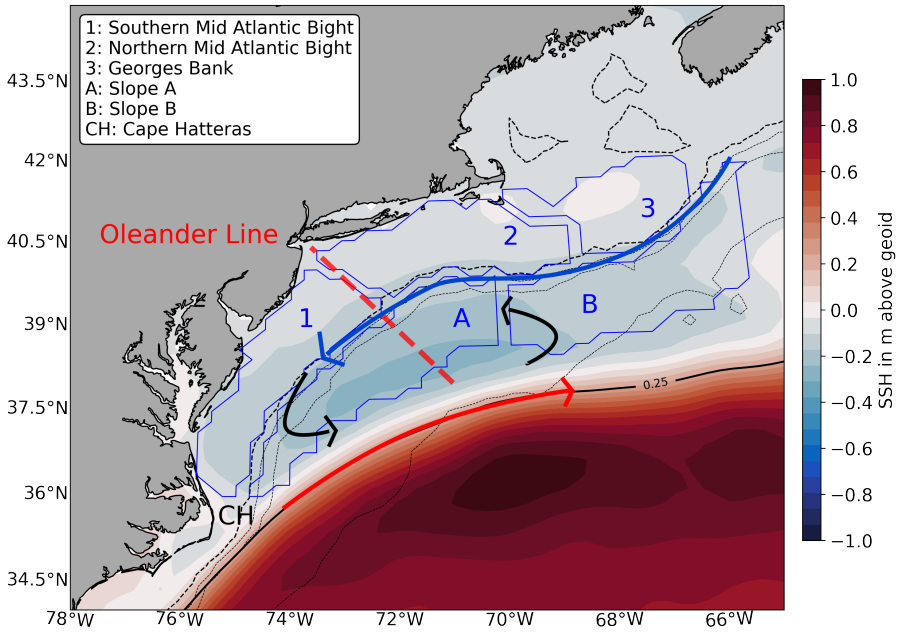

Figure 1: Map of the investigated region; Blue contours indicate shelf and slope boxes defined by *Chen et al.* (2020); Red line indicates mean track of the CMV Oleander; dashed black lines show isobaths of 200m, 1000m, 2000m and 4000m Depth; Colored is the mean absolute dynamic topography from CMEMS altimeter data for 1993 to 2019 with the 0.25m level indicated by the black line; red arrow indicates the Gulf Stream, blue the Shelf Break Jet and black the recirculation gyre

MHW formation can occur as an effect of atmosphere-ocean interactions as well as of advective processes (*Oliver et al.*, 2020). It has been shown that a MHW in this region appeared due to jet stream variability in 2012 (*Chen et al.*, 2016) and another one based on WCR interaction in 2017 (*Gawarkiewicz et al.*, 2019). Most of the research regarding MHWs is focused on the surface due to the lack of subsurface observations. In the recent years, some studies started to investigate the depth extent of MHWs and associated drivers, but still little is known. *Schaeffer and Roughan* (2017) have found MHWs in which anomalously high temperatures appeared within the full water column of 100m depth in coastal waters of eastern Australia, based on mooring data. *Elzahaby and Schaeffer* (2019) have used ARGO float data to show that MHWs can occur even at around 1000m depth. Deep events had their maximum anomalies at depth, sometimes not even occurring at the surface. They could be linked to WCRs associated to the East Australian Current, the local western boundary current. *Ryan et al.* (2020) have used a global ocean model to investigate the depth structure of Ningaloo Niño and Niña events and found that the

temperature anomalies extended to a depth of 300m or more.

This study utilizes a high resolution and eddy resolving ocean model to investigate the depth structure of MHWs in the northeast US continental shelf (Figure 1) and is divided into three parts. First, observational sea surface temperatures (SSTs) were used to detect MHWs and their trends in this region within the last four decades. The region was narrowed down to the northeast US shelf and slope region, according to ecoboxes Figure 1, defined by *Chen et al.* (2020). Local trends of duration and intensity were compared to global trends and within the shelf and slope region. The capabilities of resolving local dynamics were investigated for two simulations of a global ocean circulation model with a resolution of 1/4° and for a nest of 1/20° in the Atlantic by comparing them to observational data. The eddy resolving simulation (1/20°) was then used to describe the basic variability of temperature and salinity on the shelf according to depth, together with the mixed layer depth and ocean heat content. Therefore, one can determine multiple characteristics of MHWs. MHWs are then detected within the whole shelf region and time period. Outstanding events were selected for investigation regarding their depth structures of temperature and salinity anomalies. Three of these events were then further examined according to their 3D spatial extents and associated formation processes using surface velocities.

Therefore, the main research questions of this study are: What are the characteristics and trends of MHWs on the surface in the northeast US shelf and slope region? What effect has model resolution on representing the local dynamics? What are the depth structures of MHWs and associated formation processes?

2. Data

2.1. OISST

Optimum Interpolation Sea Surface Temperature (OISST) data is provided by the National Oceanic and Atmospheric Administration of the US (NOAA). It is based on numerous types of observations which are then combined and interpolated on a regular global grid with a resolution of 1/4°. Measurement platforms are satellites, ships, buoys and ARGO floats. Bias adjustments of satellites and ships is performed with reference to buoys (*Reynolds et al.*, 2007). Daily and monthly mean temperatures from 1982 to 2019 have been used.

2.2. Sea Surface Height

The Copernicus Marine Environment Monitoring Service (CMEMS) uses a data unification and altimeter combination system to create daily sea level products based on satellite measurements (*Rosmorduc et al.*, 2015). It resolves on a global grid of 1/4°. Monthly mean absolute dynamic topographies (Sea Surface Height (SSH) above geoid (Figure 1)) have been used beginning in January 1993 and ending in May 2019.

2.3. Oleander Line

The Container Motored Vessel CMV Oleander does weekly trips between Port Elizabeth, New Jersey and Bermuda and collects data along its path (Figure 1, red dashed line). This results in a long term depth section across the Northeast US Continental shelf and slope. Since 1977, surface temperatures and salinities were observed through bucket measurements and with a thermosalinograph from 2000 ongoing. Depth ranging temperature profiles are made with expendable bathythermographs (XBTs) along the way. A vessel mounted ADCP was added to the CMV in late 1992, generating velocity profiles. This study used the data processed by *Forsyth et al.* (2020), which consists of continuous monthly temperature sections from 1977 to 2018 on a 10km horizontal and 5m vertical resolution as well as 1362 velocity transects from 1994 to 2018 on a 4km horizontal and 8m vertical grid. The northern edge of the Gulf Stream is the southern edge of the used section as measurements south of the Gulf Stream are inconsistent (Figure 1). Velocities are rotated according to the bathymetry of the slope and the prevailing currents. This results in a southwest along shelf and a southeast cross shelf component with 225°T and 135°T respectively. This dataset is unique by providing long term observational data covering a whole section and therefore opportunities for investigation.

2.4. ORCA025

ORCA025 is an ocean global circulation model configurated by the Nucleus for European Modeling of the Ocean NEMO (code version 3.6). It runs on a global tripolar ORCA025 grid with a horizontal resolution of 1/4°, making it eddy-permitting. It consists of 46 depth levels of varying thickness from 6m at the surface to 250m at depth. Only the top 20 levels ranging from the surface to 500m depth have been used. The model run is a hindcast from 1958 to 2016 and forced at the surface by JRA-55-do v1.4. This is an atmospheric reanalysis product based on the full observing system starting in 1958 until the current day (*Tsujino et al.*, 2018; *Kobayashi et al.*, 2015). The concerning variables were monthly mean fields of SST, Mixed Layer Depth (both 2D) and 3D fields of temperature, salinity as well as zonal and meridional velocities. The Mixed Layer Depth in NEMO is defined as the depth, where the density is $0.01\,g\,kg^{-1}$ lower than at the surface.

2.5. VIKING20X

The main dataset for this thesis is output from the high resolution ocean simulation VIKING20X. It results from a nest of 1/20° resolution in ORCA025, covering the whole Atlantic Ocean from 34°S to 70°N including our region of interest. The nests boundaries are regulated by the global circulation of ORCA025 and it undergoes the same atmospheric forcing. It consists of the same depth levels as ORCA025. As a result of the extremely high resolution, VIKING20X is eddy resolving (*Rieck et al.*, 2019). The Rossby radius of deformation describes the horizontal scale at which the effects of rotation become as important as gravitational effects (*Feliks*, 1985). Hence, it is important for eddy processes. The radius ranges from 30km near Cape Hatteras to 10km at the Great Banks (*Chelton et al.*, 1998). The resolution of the nest leads to a horizontal gridspacing of around 4-5km in this region compared to the 20-25km of ORCA025. Therefore, VIKING20X can resolve almost the full spectrum of mesoscale variability and is thus a powerful tool to investigate processes on a regional scale (*Rieck et al.*, 2019). VIKING20X is an updated configuration of VIKING20, which has been shown to reproduce dynamics like the North Atlantic Current or the Deep Western Boundary Current in the North Atlantic well (*Mertens et al.*, 2014; *Breckenfelder et al.*, 2017; *Handmann et al.*, 2018). The same variables as from ORCA025 have been used as monthly mean fields for the period of 1980 to 2019.

3. Methods

3.1. Marine Heatwave Detection

Daily OISST data has been used to detect MHWs and their characteristics in the investigated region from 1982-2019. The detection was based on the definition of MHWs by *Hobday et al.* (2016, 2018). The definition states that a MHW occurs if the temperature exceeds the 90th percentile over the climatological mean for at least five consecutive days (Figure 2). However, if two MHWs of five days or more are seperated by two or less days with temperatures below the 90th percentile, it is considered as one continuous heatwave event. The whole time period of the dataset itself has been chosen as the climatological baseline. MHWs were detected within the northeast US continental shelf and slope region separately, to examine differences between the shelf and slope. The regions were limited following the shelf and slope boxes defined by *Chen et al.* (2020), which are based on physical environment, geography and ecological characteristics (*Ecosystem Assessment Program*, 2012). The 200m-isobath separates the shelf from the slope. The chosen shelf boxes for MHW detection were the southern Middle Atlantic Bight, the northern Middle Atlantic Bight and the Georges Bank. The investigated slope consisted of boxes A and B. All boxes are outlined in Figure 1. MHW detection on daily data was performed with a python algorithm, implemented by *Hobday et al.* (2016), which calculates all metrics of interest.

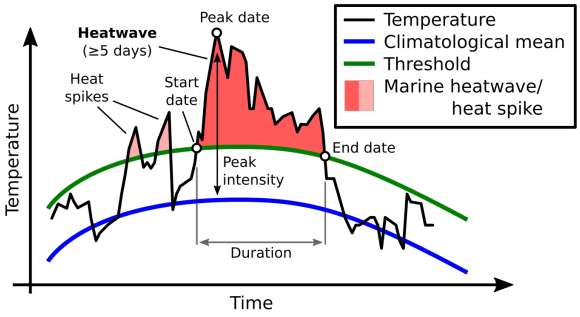

Figure 2: Schematic of the MHW definition by *Hobday et al.* (2016); figure adapted from `http://www.marineheatwaves.org/all-about-mhws.html`

Each event was characterised by duration and intensity. The intensity describes the difference between the prevailing temperature and the climatological baseline. Then, the total heatwave days per year were extracted together with the mean MHW intensity per year. A linear regression has been performed to detect and quantify trends in both of these MHW characteristics and examined for significance via a Wald Test with t-distribution. The regression was chosen to be linear to allow comparison with other studies which have used linear regression as well and for simplicity reasons. Detected MHWs were compared with the general probability distribution of temperatures according to the seasonal climatology.

3.2. Model Validation

The two simulations ORCA025 and VIKING20X were compared with observational data to test their capability to resolve the regional ocean dynamics. Based on comparability, only the overlapping time period of all data sets from 1982-01 to 2016-12 was investigated. Monthly mean SST data from ORCA025, VIKING20X and OISST was examined for surface comparison. Temperature and velocity sections measured by the CMV Oleander were compared to ORCA025 and VIKING20X. The model sections were extracted as close to the Oleander Line as the model resolutions allowed. Zonal and meridional velocities were rotated accordingly, such that they pointed in the same direction as calculated by *Forsyth et al.* (2020), e.g. south-west (along shelf) and south-east (cross shelf).

Mean and standard deviation over the whole time period were calculated for each of the examined variables and datasets and compared with the exception of salinity, as of result of there being a lack of observations regarding this variable. Both model and the observations use potential temperature. Therefore, this study refers to potential temperature using just the term temperature. The same applies for practical salinity refered to as salinity.

3.3. MHWs in VIKING20X

The MHW definition of *Hobday et al.* (2016) was applied to detect MHWs from 1980 to 2019 in VIKING20X as well. However, as monthly mean temperatures were used, each time a monthly mean temperature exceeds its specific threshold, the whole month is identified as a MHW. The threshold temperatures were calculated as the 90th percentile of a given month across all years within the datset. MHW detection was performed for each point in the models 3D space and for each timestep, which was intended to investigate the spatial distribution of MHWs over time. The investigated region was narrowed down by the same three shelf boxes (1,2,3) outlined in Figure 1 to focus on the northeast US shelf region. When analysing spatial means, thresholds were calculated again from the spatial mean temperatures to simplify the identification of temporal and spatial distribution. Temperature and salinity anomalies were determined by subtracting the mean seasonal cycle.

A detected MHW within one month does not automatically account for each day of the month being in MHW state while using monthly mean temperatures. It can also mean that there were some extremely warm days and some below the 90th percentile, but the mean still exceeds the threshold leading to a detected MHW month. As this study did not investigate one specific event or exact temporal statistics of MHWs and rather aimed for the overall spatial structure, monthly means were sufficient and simplified calculations

through smaller data volume.

After detecting all MHWs which occurred on the shelf, six larger events were selected for closer investigation due to their duration and intensity (1984-02 - 1985-06, 2002-02 - 2002-05, 2012-01 - 2012-10, 2015-03 - 2017-07. 2017-11 - 2018-02, 2019-01 - 2019-12). In the following, these events are named based on their starting year. Depth profiles of temperature and salinity anomalies, horizontally averaged for each event, were compared with the climatology and its mean variability (standard deviation of anomalies over 1980-2019).

Based on their characteristic depth structures, the events of 1984, 2012 and 2015 were chosen for even deeper investigation of their spatial and temporal distribution on the shelf and its evolution. The two months prior and post the heatwave were also analyzed to observe their formation and decay. Spatial mean temperature and salinity anomalies over time were examined further. The temporal evolution of total Ocean Heat Content (OHC) and the spatially mean Mixed Layer Depth were compared to the climatological values for each month. The OHC was calculated by integrating temperatures over space: $OHC(t) = \rho\, c_w \int\int\int T(t,x,y,z)dxdydz$. A fixed density of $\rho = 1024\, kg\, m^{-3}$ and a fixed specific heat capacity of $c_w = 3985\, J\, kg^{-1}\, K^{-1}$ were used to simplify calculations. This is valid as only the major differences between the events were of interest and not the absolute values.

MHW detection for each point in space and time lead to an array with ones if the temperature exceeds the threshold and zeros if not. This was done for the whole data period. By averaging this array over time and a weighted mean in depth, considering the difference in layer thickness, the percentage of the water column being in a MHW state could be derived. Thereby, the spatial distribution of MHWs could be determined. 100% denotes that the whole water column at a certain latitude and longitude point experienced a MHW during the whole period. This does not account for the vertical structure of the MHW, e.g. a value of 50% could indicate a heatwave state in just the upper or the lower half of the water column. Also, the MHW could start at the surface and propagate deeper over time. To examine the vertical evolution of MHWs, depth sections were extracted according to the horizontal distribution. Hence, the section covers the most impacted area of the MHW. The sections were meridionally limited according to the shelf boxes and go along 68°W, 70°W and 71.5°W for the events in 1984, 2012, 2015, respectively. Temperature and salinity anomalies along these sections were examined for each month experiencing a MHW. To investigate impacts of Gulf Stream WCRs, surface velocities were investigated for each month with underlaying MHW distribution. By this, the temporal evolution could be traced and connected with or without eddy interaction.

4. Results

4.1. Characteristics and trends of MHWs

Daily observed SST MHW detection found 71 surface heatwaves on the shelf and 57 on slope from 1982 to 2019. Each heatwave was described with its duration and its maximum, cumulative and mean intensity. However, it was not checked whether events were only on the shelf/slope or if they overlapped. Most of the events were categorised as moderate following the definition of *Hobday et al.* (2018). Some strong events occured in both regions and the severe MHW of 2012 was found as well (*Hobday et al.*, 2018).

An increase over time can be seen for nearly all of the examined MHW properties, especially starting around 2010. Figure 3 shows the total detected MHW days and the mean MHW intensity per year for shelf and slope together with their trends. The slope experienced more total MHW days than the shelf, which is dominated by MHWs in the 2010s. The trend of 32.6 ± 7.9 total days per decade is greater than the trend on the shelf of 21.3 ± 5.5 total days per decade. Both trends are significant on the 95% level.

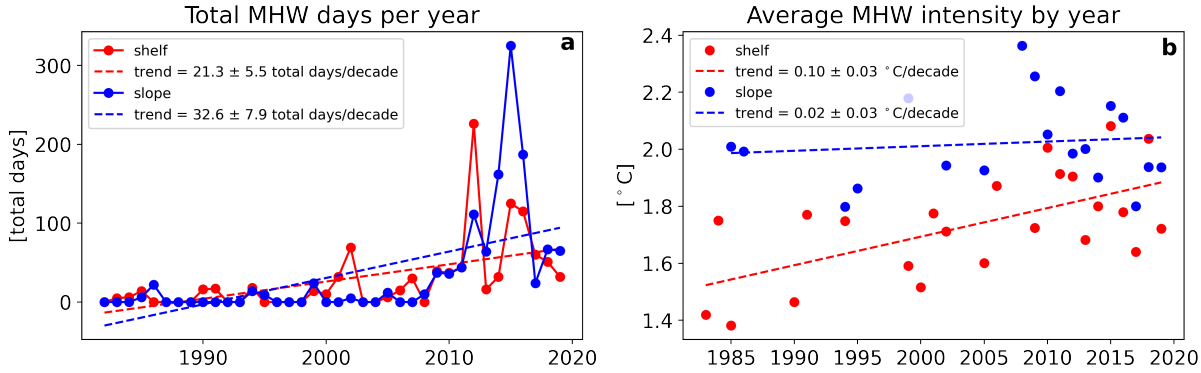

Figure 3: Total detected MHW days per year (a) and Average MHW intensity per year (b) for the shelf and slope; regions according to boxes in Figure 1; Both shelf trends and the total day trend on the slope are significant on the 95% level

Both the maximum intensity and the cumulative intensity (not shown) per heatwave show an increase too, which leads to an increase in the mean intensity as well (Figure 3b). In contrast to the total MHW days, the trend of mean intensity is much greater on the shelf, which could be due to the fact that shallower shelf waters can be influenced more by global warming than more varying slope waters. Additionally, only the trend on the shelf is significant on the 95% level. The absolute values are in contrary greater on the slope, but will balance out or become even greater on the shelf according to the trends.

Oliver et al. (2018) detected a global mean increase of 8.6 days per decade and an increase in MHW intensity of +0.085°C per decade, both significant on the 99% level. The

northeast US continental shelf region shows double the trend in MHW days and exceeds the intensity trend by 0.15°C. The slope region has three to four times the increase in MHW days whereas the intensity increase is much lower than globally. Probability distributions of temperatures relative to the climatology (Figure A1) reveal that the curve for the slope is more flattened i.e. has larger tails, which results in higher MHW thresholds when following the 90th percentile definition. This leads to a greater minimum intensity for detected MHWs and can explain the overall higher intensities on the slope. *Andres* (2016); *Gangopadhyay et al.* (2019) showed an increase in WCR activity in this region, which will increase variability by more frequently advecting warm and salty Gulf Stream waters. This can influence MHW characteristics.

This increase in occurrence and intensity of MHWs strongly highlights the need of a better understanding of MHWs and their effects on the climate and ecosystems (*Frölicher and Laufkötter*, 2018), especially in the shelf region. However, observational data such as OISST is mostly recorded at the surface and very few mooring sites exist, which provide long term measurements. In addition, many moorings at close sites would be needed to investigate overall 3D spatial extents of MHWs. These issues suggest the use of ocean models. The ability of the model to represent local dynamics is a basic condition for a meaningful investigation.

4.2. Modelled vs. observed regional hydrography

The representation of dynamics on the northeast US continental shelf region was investigated for an ocean model. Two simulations of this model have been used; ORCA025 and VIKING20X with 1/4° and 1/20° resolution, respectively. Both were compared with observations at the surface and along a depth section in respect to temperatures and velocities.

The general structure of SST in ORCA025, VIKING20X and OISST is quite similar (Figure 4a-c). However, important differences appear on the shelf break and especially around Cape Hatteras and the Great Banks. The greatest temperature gradient indicates the path of the Gulf Stream. It separates warm subtropical waters from cold polar waters, which are transported southward along the shelf by the Labrador Current and the Shelf Break Jet (*Fratantoni and Pickart*, 2007). In ORCA025, the Gulf Stream follows the coast and therefore separates too far north around 40°N. In contrast, VIKING20X does a better job leading to a Gulf Stream separation at Cape Hatteras (35°N) as in the observations. The same applies for the Great Banks, where the Gulf Stream in VIKING20X follows the continental slope around the Great Banks, whereas in ORCA025, it continues zonally

between 40°N and 45°N. These main differences are indicated by the red line in Figure 4.

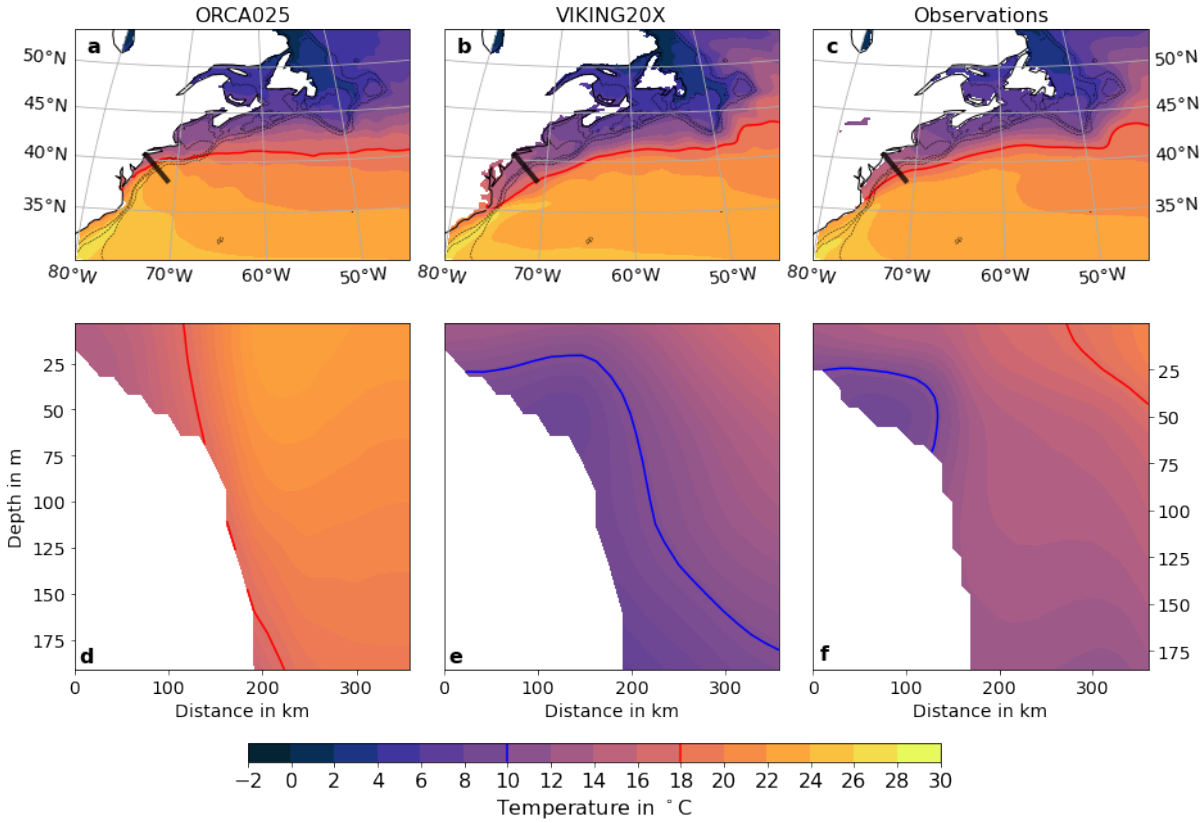

Figure 4: Mean SST (a-c) and temperature means along the Oleander Line (d-f) (marked black in a-c) for ORCA025 (a,d), VIKING20X (b,e), OISST (c) and CMV Oleander XBTs (f) for the overlapping time period from 1982 to 2016; dashed lines in a-c indicate isobaths at 100m, 500m and 2000m depth; 18°C as red contour; blue contour line in e,f at 10°C indicating cold pools; distance in d-f starts at Ambrose Lighthouse in New York Bay

These differences in the Gulf Stream path have a clear impact on the hydrography on the Northeast US continental shelf (Figure 4d-f). In ORCA025, warm Gulf Stream waters dominate the shelf and shelf break region. In contrast, the observational mean Gulf Stream path lays right at the end of the used Oleander Line. This can be seen in Figure 1 with the 0.25m contour line indicating the mean Gulf Stream path. The edge of the Gulf Stream is visible in the depth sections of VIKING20X and OISST at the outer most distances. This also turns out when investigating along shelf velocities at the Oleander Line. ORCA025 shows high northeastward velocities right around the shelf break indicating the Gulf Stream, whereas both VIKING20X and the observations show the southwestward flowing Shelf Break Jet. Another big difference between the models is the cold water pools on the shelf, which VIKING20X shows and ORCA025 does not as a result of the Gulf Stream dominance. Cold water pools are remnants of winter water being mixed downward based on strong cooling on the surface and characterised by

temperatures below 10°C (blue line in Figure 4e,f) (*Forsyth et al.*, 2015). Below that at around 100m, the Shelf Break Front occurs based on a local temperature maximum leading to a cross shelf density gradient. This front supports the southward flowing Shelf Break Jet (*Harden et al.*, 2020). The front and the cold water pool stand out more in the observations, but are visible in VIKING20X as well. However, VIKING20X shows in general colder temperatures as the observations by around 2° C.

These demonstrated differences on the shelf clearly lead to the use of VIKING20X, if one is interested to investigate dynamics and properties, of for example MHWs, on the North-east US shelf region with an ocean model. This furthermore highlights the importance of spatial resolution and the associated mesoscale resolution capabilities to resolve the ongoing ocean dynamics in this region.

4.3. VIKING20X Climatology

Before detecting MHWs on the shelf with VIKING20X, the mean states of temperature and salinity over depth and mixed layer depth on the shelf were investigated (Figure 5a,b). This shows the overall means and standard deviations, e.g. including the seasonal cycle. As expected, temperature decreases with depth by around 4°C and varies the most at the surface. However, the local temperature maximum below 100m depth indicates the Shelf Break Front, which shows the influence of warmer slope waters. Salinity increases by 4psu from the surface to 160m depth, but its variability changes minimally. The mixed layer depth is influenced by both of these properties and its variability is dominated by the seasonal cycle (not shown, indicated by standard deviation), being shallower in summer and deeper in winter. Differences in temperature and salinity occur when examining the seasonal cycle. The temperature is most stratified in summer and least in winter, due to surface cooling. Convection over winter leads to the overall coldest temperatures during spring. Summer surface warming mixes downward during fall. The salinity stays nearly the same at the bottom during the whole year. *Richaud et al.* (2016) showed that increased river runoff leads to a freshening of around 1psu at the surface in summer.

Both temperature and salinity show trends over the whole period, which vary over depth (Figure 5c,d). Temperature shows a warming of 1.5°C at the surface, which increases with depth up to a maximum of 4°C at around 140m, then decreases with depth. Salinity shows the same depth structure, but actually a freshening of 0.3psu at the surface and a maximum increase at 125m depth of 0.5psu. These trends at depth match the results of *Saba et al.* (2015) and *Gawarkiewicz et al.* (2018), who show a northward shift of the Gulf Stream and additional associated WCR interactions intruding warmer and saltier

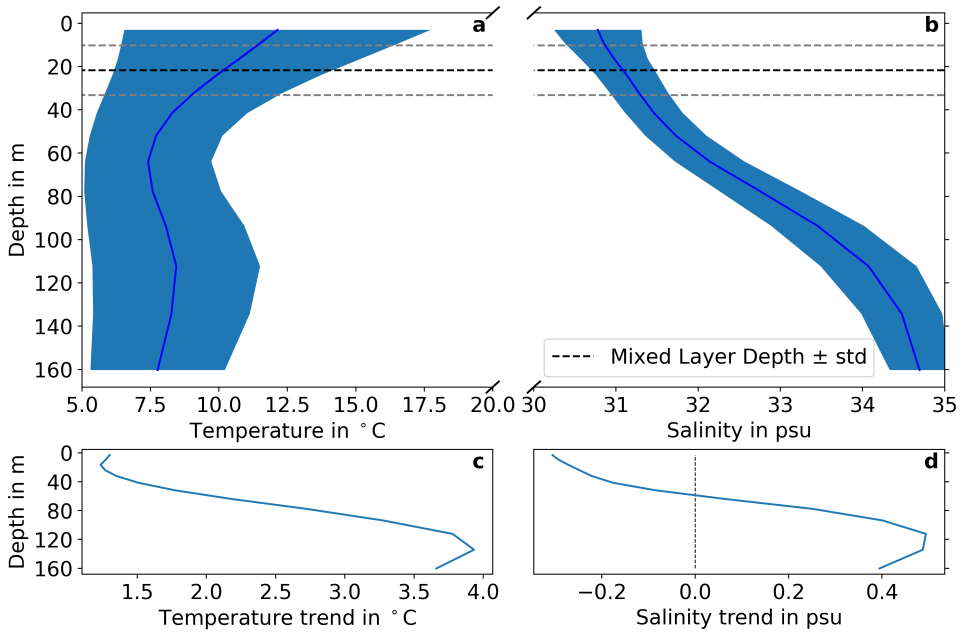

Figure 5: Temporal and horizontal means and standard deviations for temperature (a), salinity (b) and mixed layer depth (a,b) plus spatial mean temperature (c) and salinity (d) trends over the whole shelf region (Figure 1) for the whole time period

water more frequently on to the shelf. The freshening at the surface could be a result of increased river runoff, a signal of melting ice sheets in the arctic or a decrease in salt input somewhere on the path of the water masses reaching the US continental shelf.

4.4. MHWs on the shelf

By detecting MHWs for every point in 3D model space, their spatial structure and their evolution could be evaluated. Figure 6 shows horizontal mean temperature (a) and salinity anomalies (b) over depth and time. Detected MHWs are outlined with black contour lines. Varying depth structures occur with some heatwaves being entirely subsurface, some only at the surface and some over the entire water column. It is noticeable that MHW thresholds are varying for each depth. Below 100m depth, some temperature anomalies are greater and not associated with a MHW compared to MHWs on the surface with lower absolute anomalies. The highest temperature anomalies appear around 100m depth with up to 8°C. In contrast, one might suspect cold spells as well, based on high cold anomalies e.g. around 1996. These are the inverse phenomenon to of MHWs, but were not investigated in this study.

Salinity anomalies appear to positively correlate with temperatures at first. But there are some surface events with a negative anomaly (2002 & 2012). Furthermore, some high

salinity anomalies occur which are not associated to a MHW (early 1980s). Temporally, an increase of MHWs appears post 2010, matching the results found in Section 4.1. However, one event stands out at the start of the time series around 1984, which occurred prior to the influence of the warming trend and is therefore of great interest.

It needs to be mentioned that based on the bathymetry of the shelf, spatially averaged surface values belong to much more data points, e.g. a greater area, than values at greater depth. Because of that, percentage distributions were calculated, showing how much of the entire shelf at a certain depth experiences a MHW (Figure A2). Results show the same general structure of MHWs as Figure 6, but indicate their core depths. These relations of temperature and salinity for MHWs suggest different drivers, which will be more closely examined later in this study. In the horizontally averaged temperature anomalies, 48 months in total are associated with a MHW at the surface as well as at 100m depth. The specific months differ between the surface and depth as visible in Figure 6.

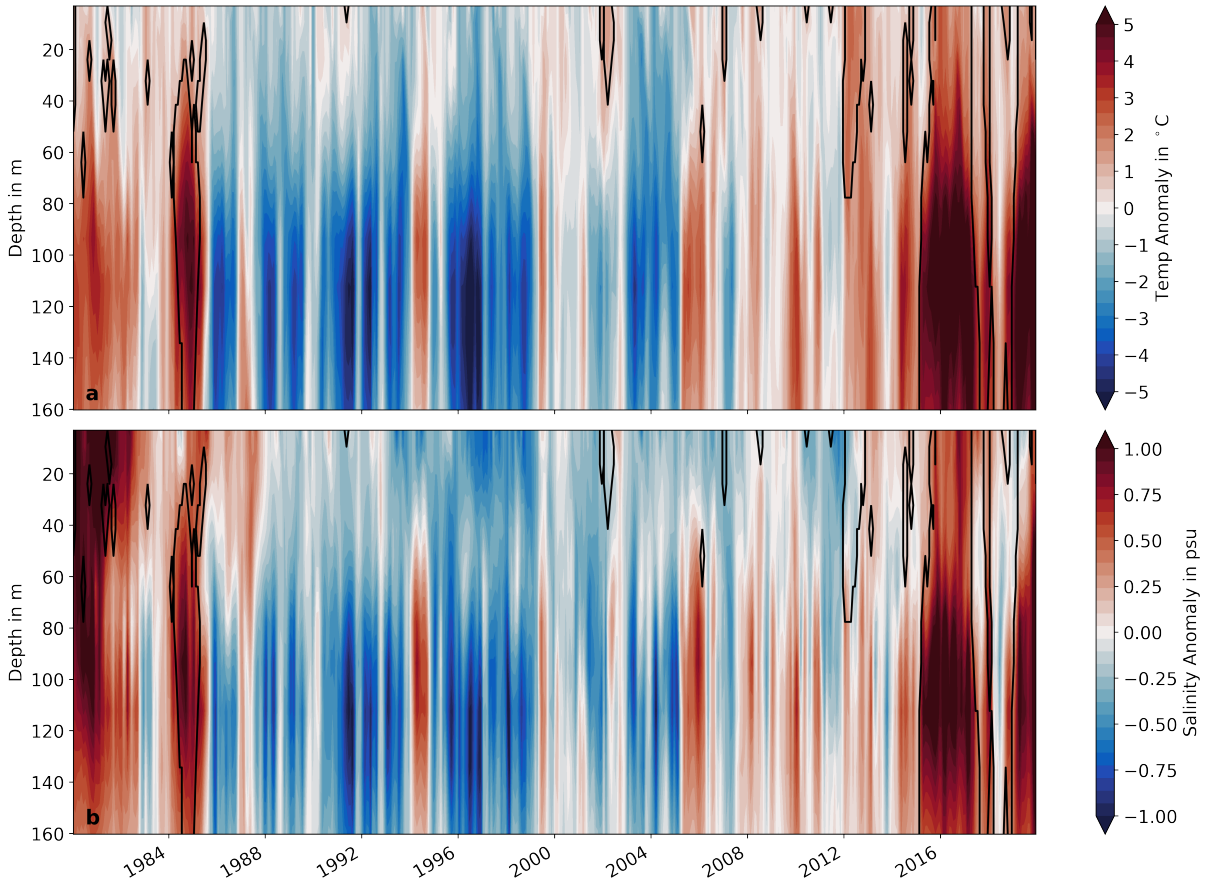

Figure 6: Spatial mean temperature (a) and salinity anomalies (b) over depth and time for the whole shelf region; black contour lines indicate MHWs

4.5. Depth structure and associated drivers

Six events were selected based on their different structures (see Section 3.3 for their chosen dates). These events vary between their lengths and the according seasons. Depth profiles of temperature anomalies averaged over time and space for each of the considered events are shown in Figure 7a. The events of 1984, 2015, 2017 and 2019 show overall similar profiles with their maximum anomaly located at around 100m depth and lowest at the surface. 2002 and 2012 have their maximum at the surface and then decreasing constantly with depth. In 2002, anomalies actually inverse over depth being negative below 50m. The anomalies of 2012 do not really change with depth, but only the upper 80m exceed the MHW threshold. These events show discrepancies in Ocean Heat content of the entire shelf averaged over the MHW period. The total spatial Ocean Heat Content of 2002 is only 75% of the mean state, due to the cold anomalies at depth. All the other events are greater with up to 120% of the mean, the highest are 2019, 2015 and 2012. This is not the best measure as it highly depends on spatial distribution of each MHW, but it still shows impacts of MHWs.

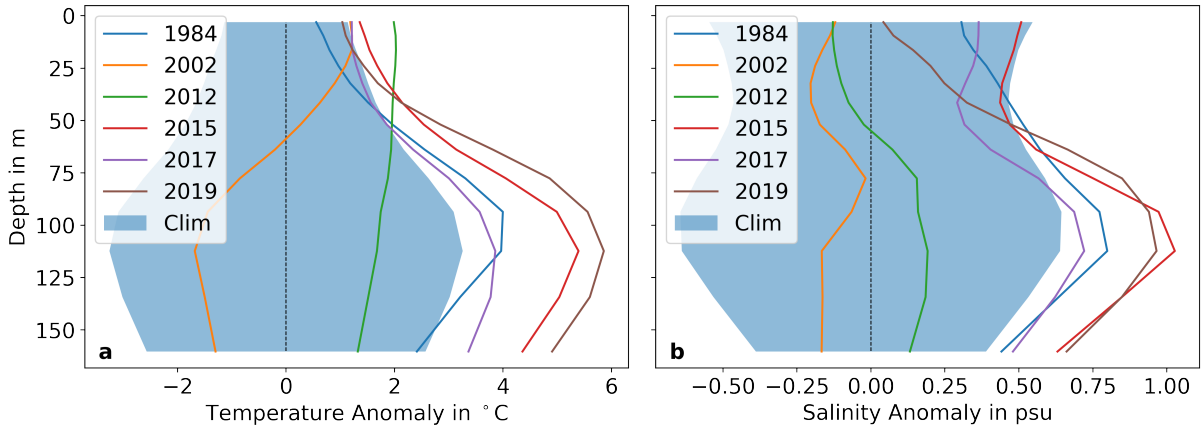

Figure 7: Profiles of mean temperature (a) and salinity anomaly (b) for six events in comparison to the climatology (blue shading denotes ±1 std)

Figure 7b shows the depth profiles of salinity for the same events. 1984, 2015, 2017 and 2019 show similar structures as for temperature anomalies with their maximum at around 100m depth. The surface values vary more between each event than they did for temperature. 2002 and 2012 show a small freshening at the surface. However, 2012 changes to positive anomalies over depth and 2002 remains almost the same.

The three events of 1984, 2012 and 2015 were selected for even further investigation concerning their temporal evolution of spatial structure and indicating possible drivers. The three events show very different depth profiles with either being only subsurface, only at the surface or over the entire water column. Figure 8 shows the spatial distribution

(a,d,g) for each event plus their temperature (b,e,h) and salinity anomalies (c,f,i) over time.

Starting with 1984 (Figure 8a-c), one can see that the heatwave only occurs beneath the surface below 40m depth with the strongest anomalies of 5°C at 100m depth. This is also visible in the distribution, where the MHW dominates the shelf break region. The shallower parts near the coastline are not impacted except for some deeper channels, e.g. at 69°W. Differences also occur horizontally with the region between the northern Middle Atlantic Bight and the Georges Bank is affected the most. The MHW has a time span of one year.

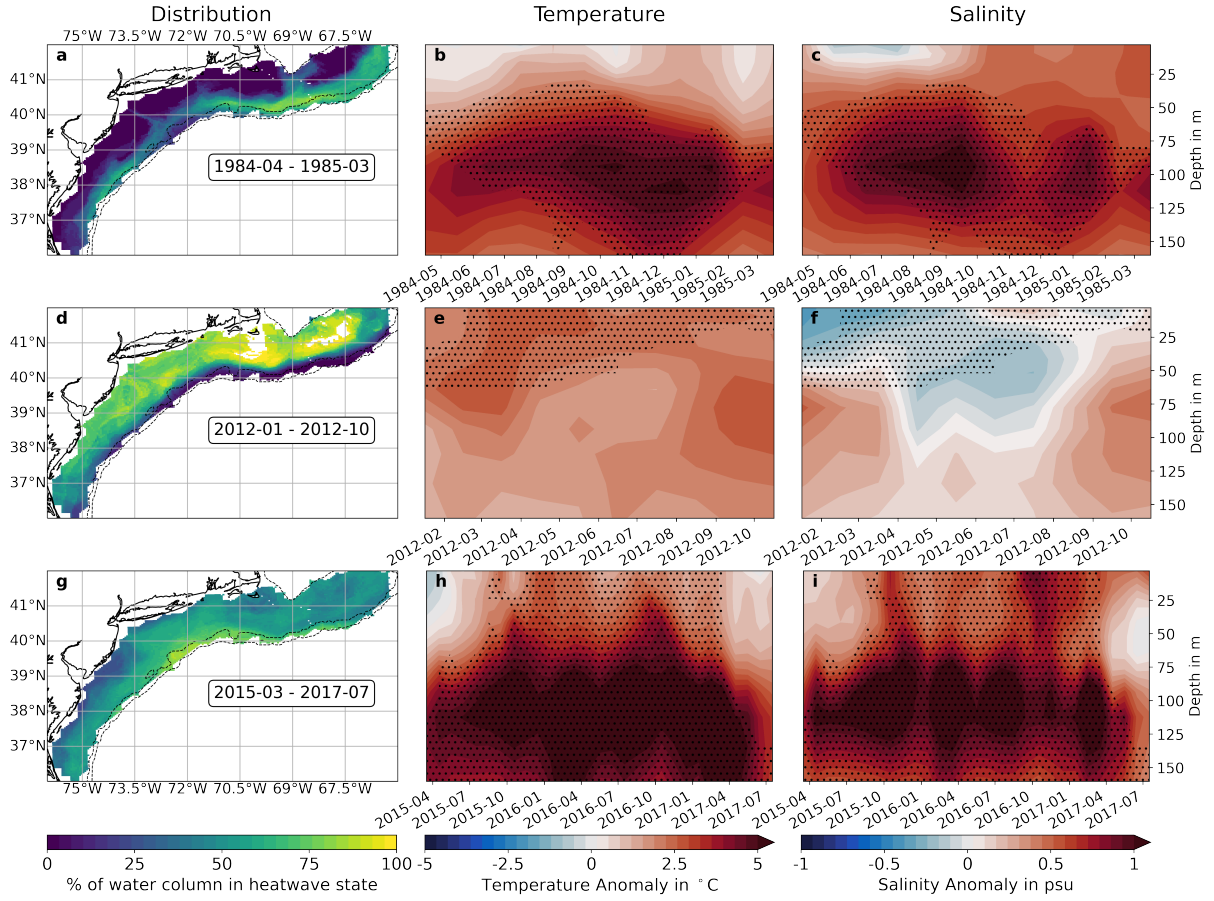

Figure 8: Distribution (a,d,g) and horizontal mean temperature (b,e,h) and salinity anomalies (c,f,i) over depth for the MHWs of 1984 (a-c), 2012 (d-f) and 2015 (g-i); black contour lines in left column are isobaths of 100m and 500m depth; hatching in mid and right column indicates MHW state (exceeding 90th percentile for each point)

The MHW does not occur according to an absolute anomaly threshold, which results from the comparison of temperature anomalies and the MHW state. This underlines that each depth has its own specific climatology and therefore its 90th percentiles defining MHWs. Salinity anomalies show a very similar structure during the whole MHW with

maximum anomalies of 1psu, although the temporal development is different. The overall mixed layer depth is not really different to the climatological variability within this entire heatwave. The total OHC of the shelf is greater than one standard deviation of the monthly climatological mean from June 1984 to February 1985.

A meridional section along 68°W was selected together with the horizontal MHW distribution and surface velocities for each month (not shown) to determine the temporal evolution. The 1984 MHW propagated from the most eastern edge of the Georges Bank to the southern end of the Middle Atlantic Bight following the shelf break. It reaches the southern tip in November 1984 and starts to decay in the north on the Georges Bank in February 1985. At the section, the anomalies show the same overall structure. The MHW is focused on the shelf break never reaching regions with a maximum depth of 40m. However, some strong anomalies appear at the surface which also exceed the MHW threshold. At this point, to clarify possible confusion, the differences of calculation between the plots need to be mentioned again. The anomalies of Figure 6 and Figure 8 as well as their MHW thresholds are based on the horizontal spatial means over the whole shelf region. Some local MHWs structures, as in the section, may not be strong or spatially spread enough and are therefore averaged out. These detailed spatial structures were not further investigated as this study gives an overview about MHWs and their depth structure and did not intend to determine the exact spatial development of one certain event, which would require a much closer look into the 3D velocity field.

The MHW of 2012 (Figure 8d-f) is a surface heatwave only reaching deep to a depth of 60m, being quite the opposite to 1984. Furthermore, it is focused on the shallower shelf without influencing the shelf break at all. Its main regions are the north eastern Middle Atlantic Bight and the Georges Bank. However, the whole investigated shelf region is impacted by the MHW. The MHW has a length of ten months. Absolute temperature anomalies are not as strong as in 1984, the maximum is 2.5°C. Salinity anomalies are negative in the upper parts of the water column. The high surface anomalies lead to a shallower mixed layer depth during winter and spring based on additional stratification, exceeding one standard deviation. The OHC is greater than one standard deviation from December 2011 until December 2012. The temporal evolution of distribution shows that the MHW started on the coast of the whole region in December 2011. It then extended on to the entire shelf within three months. The decay started in July 2012 and ended in November. The temporal evolution of anomalies is determined from a depth section at 70°W. This highlights, that the MHW takes place only on the shallow shelf regions, but then impacting the entire water column. Salinity anomalies are negative during the whole time, but start to become positive at the end of the event.

The MHW of 2015 (Figure 8g-i) is by far the strongest event detected with temperature anomalies up to 8°C. It has a time span of two years and 3 months. The entire region and the whole water column is impacted. The distribution shows that the shelf break region is influenced the most. The highest anomalies for temperature as well as for salinity are located at around 100m depth showing a similar pattern, especially at depth. Salinity anomalies go up to 1.5psu. The mixed layer depth is minimally influenced as the anomalies are mostly at depth. The OHC is greater than one standard deviation from July 2015 to May 2017. The mean anomalies (Figure 8h,i) already show a temporal evolution, indicated by the hatched MHW state over time. The MHW starts at 100m depth and then extends to the surface, where the decay begins as well. The same pattern is visible at a section at 71.5°W. The anomalies are highest at depth on the shelf break and then propagate shore-ward and upward. During some months, a surface heatwave appears as well which then connects to the deeper parts. However, the highest anomalies are focused on the bottom and especially on the shelf break for most of the time.

The MHW of 2019 has properties showing some sort of a mixture of 1984 and 2015 (Figure A3). It is focused at 100m depth and on the outer parts of the shelf without reaching the coastline. A propagation of anomalies from the slope sea onto the shelf break and further shore-ward describes the main temporal development. The MHW may have continued even longer if the model run did.

These connections of temperature and salinity anomalies and their spatial development suggest varying drivers for these events. The two major drivers in this region are ocean atmosphere interactions and advective processes due to the strong eddy variability (*Holbrook et al.*, 2019). Gulf Stream warm core rings (WCRs) can carry warm and salty subtropical waters to the shelf and slope region. *Hu et al.* (2016) show a poleward shift of the Gulf Stream due to climate change, which could result in additional WCRs reaching the shelf and possibly fueling MHWs. Two examples were chosen to show a MHW with WCR interaction and one without.

Figure 9 shows the formation of the MHW in 2012. Surface velocities together with MHW distribution (a-c) for three months plus temperature (d-f) and salinity anomalies (g-i) along a section reveal the temporal development. Clearly visible is a WCR in the slope sea, which is under MHW state, as it carries water being anomalously warm for this region. Much of the shelf region already undergoes a MHW in January, most likely driven by air-sea heatflux (*Chen et al.*, 2016). In the section, high temperature and salinity anomalies appear at the southern end, which are typical properties of a WCR. They extend furthest onto the shelf at depth of 60m to 80m, which could be due to the Shelf Break Jet flowing southwestward and blocking WCR waters at the surface (*Forsyth et al.*,

2020). Everything above 60m is in MHW state in January. However in February, as the WCR passed by, only the shallower parts of the shelf remain in a heatwave state. Cold and fresh anomalies can be seen at the shelf break and offshore of it, suggesting that the eddy was not able or close enough to intrude its properties on the shelf. Furthermore, the horizontal distribution of the MHW increases, which now affects the entire shelf. The same picture reveals itself in March, where the temperature anomalies near the coast increase even more, which can not have been an impact of WCR waters.

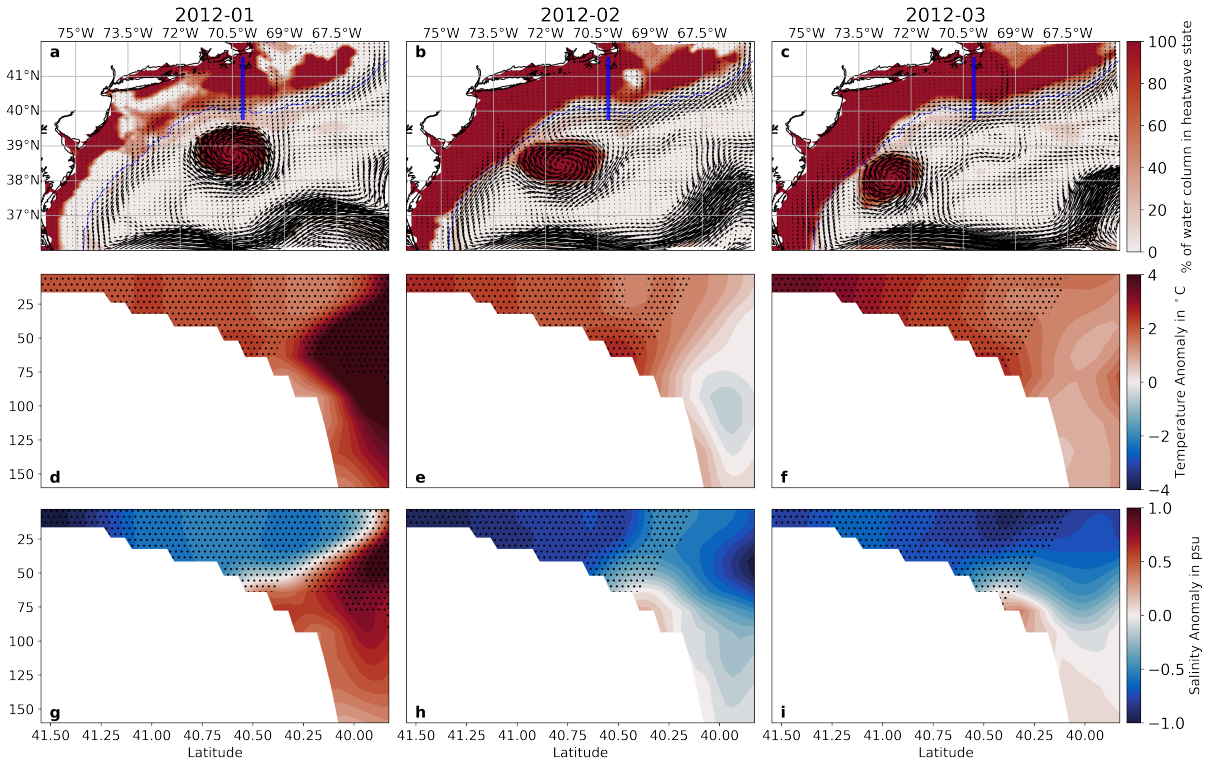

Figure 9: Horizontal surface velocities with MHW distribution (a-c), temperature (d-f) and salinity anomalies (g-i) along the blue section marked in the first row for selected months of 2012; the blue contour line in a-c indicates isobath of 200m depth; hatching in d-i indicates MHW state

The opposite occurs during the formation in 2015 (Figure 10). Once again, an approaching eddy is visible in the velocity field in all three months, bringing anomalies onto the shelf. According to the 200m isobath indicating the shelf break, this WCR propagates closer to the shelf break than in 2012, supporting interactions of ring and shelf water. In July, high anomalies can already be seen based on previous processes. But as the eddy propagates closer to the section, the anomalies at 75-100m depth propagate shore-ward and increase at the edge of the section. Temperature and salinity are affected in the same way, underlining that the WCR advects its properties on to the shelf. In comparison to 2012, surface velocities show a poleward shift of the Shelf Break Jet, which could support

this interaction by not blocking it anymore. The displacement of the Shelf Break Jet is perhaps even caused by the WCR in the first place. *Forsyth et al.* (2020) has shown effects of WCRs on Shelf Break Jet variability. During August, the surface also turns into MHW state, maybe due to atmospheric processes. Both the surface warming and the entering warm core waters lead to the subsequent MHW in the whole water column, which ongoing formation can be seen in September.

WCR interaction occurs in 2019 as well. Extreme anomalies enter the shelf at depth and propagate further on to the shelf as a WCR passes, leading to a subsurface MHW. This highlights the possibilities of WCRs fueling MHWs at depth on the shelf.

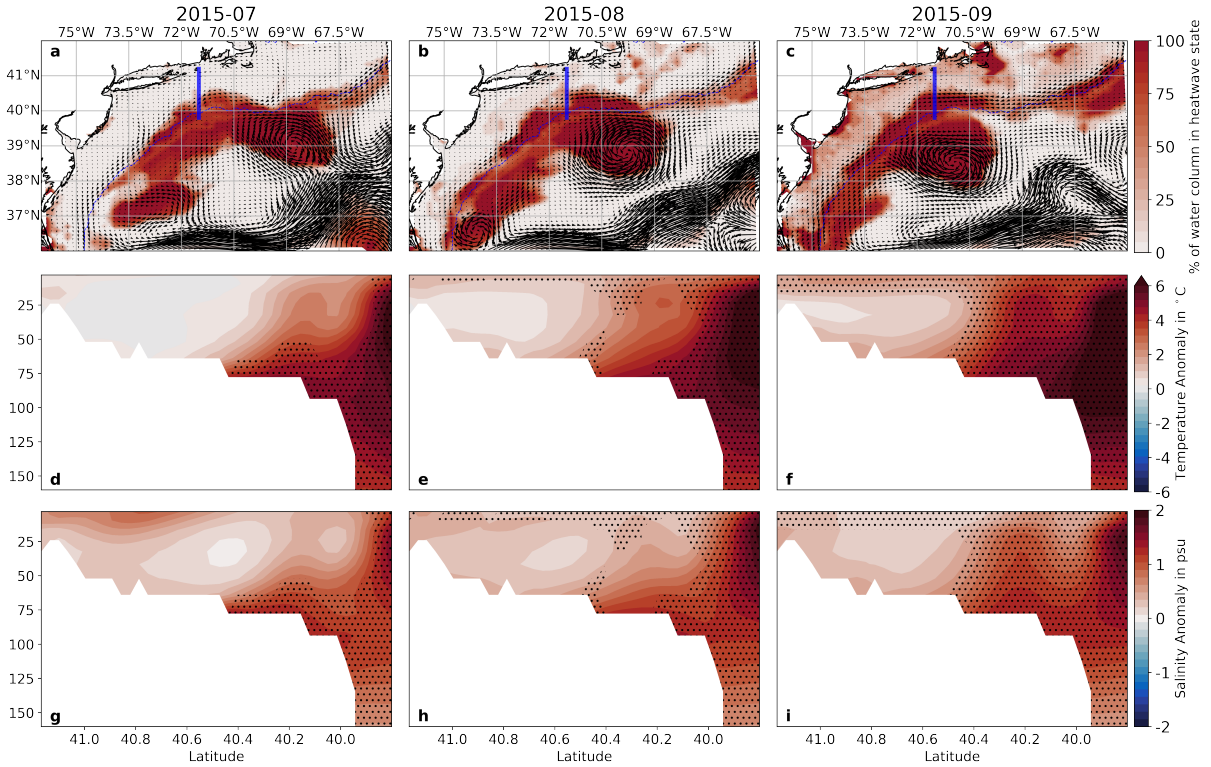

Figure 10: Same as Figure 9, but for three months of 2015

5. Discussion

First, a significant increase in occurrence, duration and intensity of MHWs on the northeast US continental shelf has been shown, especially starting in 2010. This matches the results of *Oliver et al.* (2020), who describe a global increase in MHW frequency and an increase of intensity in the western boundary current regions. The trends detected in the shelf region exceed global averages found by *Oliver et al.* (2018). This once again shows the need to better understand MHWs and their possible impacts on ecosystems. *Wernberg et al.* (2013) and *Wernberg* (2020) describe an example in Western Australia, where a MHW in 2011 completely shifted an ecosystem, which is still remaining in that new state until today and long after the MHW has decayed. Therefore, it is necessary to investigate the circumstances under which a MHW can have substantial impacts on the environment. Furthermore, local businesses such as fisheries can be affected either during the MHW or substantial as well, which could lead to economic problems (*Frölicher and Laufkötter*, 2018; *Mills et al.*, 2013). Additionally, MHWs in this region may have impacts on hurricanes, as sea surface temperatures influence the formation or decay of hurricanes (*Shapiro and Goldenberg*, 1998).

Increased knowledge about MHWs can perhaps improve the handling of MHWs or maybe even prevent these kind of impacts, if one could predict upcoming MHWs. An important point for MHW detection is the chosen baseline period and the influence of global warming. When keeping the same baseline period, the whole ocean will be in a MHW state at some point (*Oliver et al.*, 2020). This study uses the whole data period as the baseline, which averages out the warming somewhat in threshold calculation, but still leads to pronounced MHW detection at the end of the period.

The main focus of this study is the depth structure of MHWs. Due to the lack of subsurface observations, an ocean model was used to investigate this question. It turns out, that MHWs can have all sorts of spatial structures. Some events occur at the surface and in the mixed layer, whereas other events only take place at depth affecting the bottom of the water column without reaching the surface. Furthermore, events occur covering the whole water column. The depths of the highest anomalies differ between these events, while the strongest anomalies appear at depth at the shelf break. Temperature anomalies can be as high as 8°C above the climatological mean. As in the observations, a trend in frequency and intensity occurs with the main increase starting in 2010, indicating the influence of the chosen baseline. The longest event detected lasted for two years and four months.

However, monthly mean temperatures were used. Due to averaging, a MHW with high

intensity for half of the month could bring the mean value over the threshold. The threshold itself could be different as well. That is why the detected events may not be one prolonged event based on the general definition of *Hobday et al.* (2016), but many short and intense events during that period. This becomes important in the investigation of possible environmental and ecosystem impacts but also seasonal variabilities. Short but more intense events can have different influences on organisms than long events with lower intensity, which depends on the organisms physiological thermal thresholds and acclimation or adaptation capabilities (*Frölicher and Laufkötter*, 2018). These impacts on marine ecosystems need to be examined further, and due to the different depth structures of MHWs, especially on benthic and pelagic ecosystems.

Another question is whether the definition by *Hobday et al.* (2016) is also valid for subsurface MHWs. Variability in the deep sea occurs on slower timescales than on the surface (*Meinen et al.*, 2020). This may influence the minimum period of consecutive days exceeding the MHW threshold needed to define it as a MHW. However, as the shelf in this region only goes as deep as 200m and monthly means were used, this effect could be neglected in this study. *Elzahaby and Schaeffer* (2019) revealed, that SST measurements are insufficient to describe and detect each MHW, which is highlighted by this study.

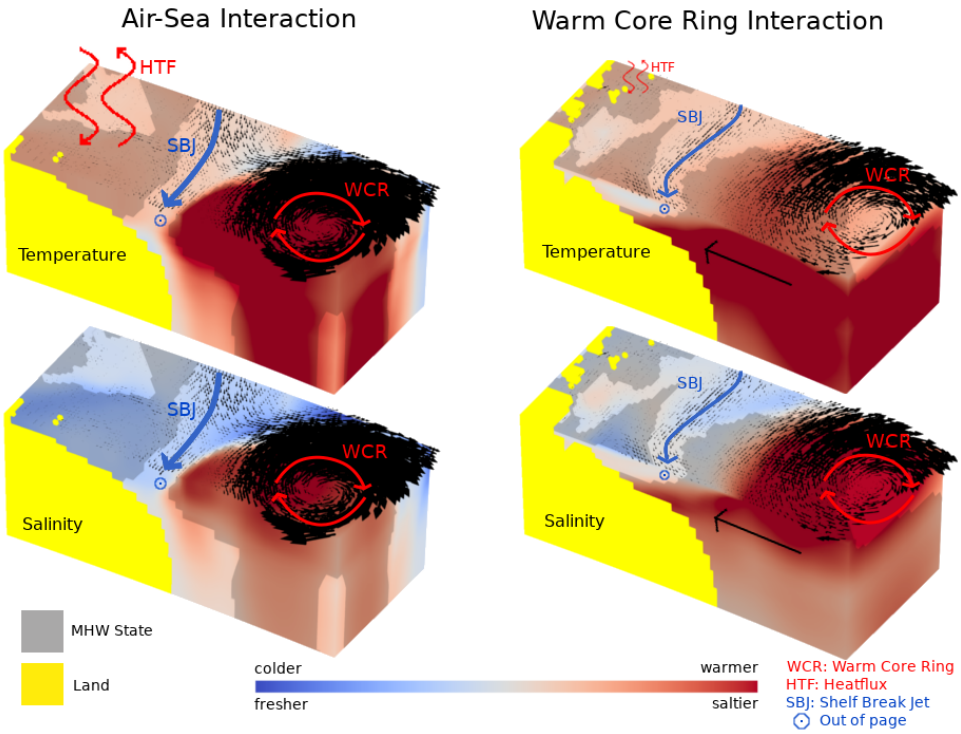

Figure 11: Schematic of MHW structure and related drivers; 3D fields of temperature and salinity anomalies and surface velocities

The different types of events were associated with different salinity anomalies. Surface events were not connected with similar salinity anomalies, whereas events at depth at the shelf break showed high salinity anomalies with the same structure as temperature anomalies (Figure 11). These discrepancies suggest varying drivers and different water masses involved during these events. MHWs at depth could be linked to Gulf Stream WCRs interacting with the shelf break. WCRs propagating close to the shelf break can be able to intrude their properties on to the shelf. *Gawarkiewicz et al.* (2018) showed an increase of frequency and onshore penetration in recent decades, which may fuel additional subsurface MHWs on the shelf. This is influenced by the relatively high temperature and salinity trends at depth at the shelfbreak, which again emphasizes the discussion regarding MHW detection baselines. Figure 11 indicates effects of the Shelf Break Jet which is blocking WCR water at the surface. Surface MHWs therefore showed no influence of WCRs and were most likely driven by atmosphere ocean interactions. This mechanism was not investigated in-depth which needs to be pursued further. An option would be to define water masses such as slope, shelf or WCR waters by temperature and/or salinity ranges and trace them during MHW formation.

There are much more dynamics which may influence the formation of MHWs, including other advective processes in both the horizontal and vertical direction, mixing and induction (*Oliver et al.*, 2020). These processes differ globally between coastal regions. This underlines the need of understanding the prevailing dynamics in the region of interest to be able to explain MHWs, already emphasized by *Schaeffer and Roughan* (2017). As described by *Andres* (2016), the Gulf Stream destabilization point shifted westward, which could be related to the recent enhanced warming on the shelf. More WCRs are occurring since 2000 (*Gangopadhyay et al.*, 2019). This indicates the possible impacts of climate change on local dynamics and therefore MHW formation. Atmosphere-ocean interactions can drive MHWs as well through varying heat fluxes or wind caused downwelling (*Chen et al.*, 2016; *Schaeffer and Roughan*, 2017).

As VIKING20X is an ocean only model, it is hard to investigate impacts of two sided ocean atmosphere interactions which may affect MHWs. It may be the ocean can trigger an atmospheric heatwave as well. However, as the simulation is forced by observed/reanalysed heat and momentum fluxes at the surface, interactions can be examined but were only assumed within this study. Coupled climate models would be an option to examine this further. Another interesting option would be coupled ocean and biogeochemical models to investigate impacts on ecosystems.

The effect of model resolution in resolving the prevailing dynamics for the shelf and slope in the Gulf Stream region has been proven. Clear differences appear between ORCA025

and VIKING20X with 1/4° and 1/20° resolution, respectively. VIKING20X shows known properties of the northeast US continental shelf region such as the Shelf Break Jet, the Shelf Break Front and cold pools, matching the observations and findings by *Forsyth et al.* (2020) and *Gawarkiewicz et al.* (2018). The shelf in ORCA025 on the other hand is highly dominated by the Gulf Stream itself, which separates too far north of Cape Hatteras to then flow on the shelf break. Therefore, VIKING20X demonstrates the need for a model's ability to reproduce mesoscale variability through high resolution by lowering horizontal grid spacing below the Rossby radius of deformation. However, the techniques to show these discrepancies were very basic in this study. That is why additional model validation is needed to further investigate the capabilities of VIKING20X apply founded results to the reality with more confidence. Additionally, VIKING20X showed offsets of absolute values to the observations which needs to be considered and examined.

In conclusion, this study shows that MHWs can occur with all types of depth structures, which then can result in impacts on different ecosystems. Different structures can be linked to varying drivers, which are highly dependant on the local dynamics of the investigated region. The study highlights the need of continuous long term subsurface observations, while revealing the capabilities of high resolution ocean models to investigate MHWs.

6. References

Andres, M. (2016), On the recent destabilization of the Gulf Streampath downstream of Cape Hatteras, *Geophysical Research Letters*, *43*, 9836–9842, doi:10.1002/2016GL069966.

Breckenfelder, T., M. Rhein, A. Roessler, C. W. Böning, A. Biastoch, E. Behrens, and C. Mertens (2017), Flow paths and variability of the North Atlantic Current: A comparison of observations and a high-resolution model, *Journal of Geophysical Research: Oceans*, *12*(4), 2686–2708, doi:https://doi.org/10.1002/2016JC012444.

Chelton, D. B., R. A. Deszoeke, M. G. Schlax, K. El Naggar, and N. Siwertz (1998), Geographical variability of the first baroclinic Rossby radius of deformation, *Journal of Physical Oceanography*, *28*(3), 433–460, doi:10.1175/1520-0485(1998)028<0433:GVOTFB>2.0.CO;2.

Chen, K., Y. O. Kwon, and G. Gawarkiewicz (2016), The role of atmospheric forcing versus ocean advection during the extreme warming of the Northeast U.S. continental shelf in 2012, *Journal of Geophysical Research: Oceans*, *121*(9), 6762–6778, doi:10.1002/2016JC011646.

Chen, Z., Y. O. Kwon, K. Chen, P. Fratantoni, G. Gawarkiewicz, and T. M. Joyce (2020), Long-Term SST Variability on the Northwest Atlantic Continental Shelf and Slope, *Geophysical Research Letters*, *47*(1), 1–11, doi:10.1029/2019GL085455.

Csanady, G. T., and P. Hamilton (1988), Circulation of slopewater, *Continental Shelf Research*, *8*(5-7), 565–624, doi:10.1016/0278-4343(88)90068-4.

Ecosystem Assessment Program (2012), Ecosystem Status Report for the Northeast Shelf Large Marine Ecosystem - 2011, *US Deptartment of Commerce, Northeast Fish Sci Cent Ref Doc. 12-07*, *1*(April), 32p.

Elzahaby, Y., and A. Schaeffer (2019), Observational Insight Into the Subsurface Anomalies of Marine Heatwaves, *Frontiers in Marine Science*, *6*(December), 1–14, doi:10.3389/fmars.2019.00745.

Feliks, Y. (1985), On the Rossby Radius of Deformation in the Ocean, *Journal of Physical Oceanography*, *15*(11), 1–16, doi:https://doi.org/10.1175/1520-0485(1985)015<1605:OTRROD>2.0.CO;2.

Forsyth, J., M. Andres, and G. Gawarkiewicz (2020), Shelfbreak Jet Structure and Variability off New Jersey Using Ship of Opportunity Data From the CMV Oleander, *Journal of Geophysical Research: Oceans*, pp. 1–19, doi:10.1029/2020JC016455.

Forsyth, J. S. T., M. Andres, and G. G. Gawarkiewicz (2015), Recent accelerated warming of the continental shelf off New Jersey: Observations from the CMV Oleander expendable bathythermograph line, *Journal of Geophysical Research C: Oceans*, *120*(3), 2370–2384, doi:10.1002/2014JC010516.

Fratantoni, P. S., and R. S. Pickart (2007), The western North Atlantic shelfbreak current system in summer, *Journal of Physical Oceanography*, *37*(10), 2509–2533, doi:10.1175/JPO3123.1.

Frölicher, T. L., and C. Laufkötter (2018), Emerging risks from marine heat waves, *Nature Communications*, *9*(1), 2015–2018, doi:10.1038/s41467-018-03163-6.

Gangopadhyay, A., G. Gawarkiewicz, E. N. S. Silva, M. Monim, and J. Clark (2019), An Observed Regime Shift in the Formation of Warm Core Rings from the Gulf Stream, *Scientific Reports*, *9*(1), 1–9, doi:10.1038/s41598-019-48661-9.

Gawarkiewicz, G., R. E. Todd, W. Zhang, J. Partida, A. Gangopadhyay, M.-U.-H. Monim, P. Fratantoni, A. Malek Mercer, and M. Dent (2018), The Changing Nature of Shelf-Break Exchange Revealed by the OOI Pioneer Array, *Oceanography*, doi:10.5670/oceanog.2018.110.

Gawarkiewicz, G., et al. (2019), Characteristics of an Advective Marine Heatwave in the Middle Atlantic Bight in Early 2017, *Frontiers in Marine Science*, *6*(November), 1–14, doi:10.3389/fmars.2019.00712.

Handmann, P., J. Fischer, M. Visbeck, J. Karstensen, A. Biastoch, C. Böning, and L. Patara (2018), The Deep Western Boundary Current in the Labrador Sea From Observations and a High-Resolution Model, *Journal of Geophysical Research: Oceans*, *123*(4), 2829–2850, doi:https://doi.org/10.1002/2017JC013702.

Harden, B. E., G. G. Gawarkiewicz, and M. Infante (2020), Trends in Physical Properties at the Southern New England Shelf Break, *Journal of Geophysical Research: Oceans*, *125*(2), 1–12, doi:10.1029/2019JC015784.

Hobday, A., et al. (2018), Categorizing and Naming Marine Heatwaves, *Oceanography*, *31*(2), 162–173, doi:10.5670/oceanog.2018.205.

Hobday, A. J., et al. (2016), A hierarchical approach to defining marine heatwaves, *Progress in Oceanography*, *141*, 227–238, doi:10.1016/j.pocean.2015.12.014.

Holbrook, N. J., et al. (2019), A global assessment of marine heatwaves and their drivers, *Nature Communications*, *10*(1), 1–13, doi:10.1038/s41467-019-10206-z.

Hu, Y., L. Gerrit, W. Wei, D. Mihai, I. Monica, and L. Jiping (2016), Intensification and

poleward shift of subtropical western boundary currents in a warming climate, *Journal of Geophysical Research: Oceans*, *121*(5), 3010–3028, doi:10.1002/2015JC011513.

Jones, T., et al. (2018), Massive Mortality of a Planktivorous Seabird in Response to a Marine Heatwave, *Geophysical Research Letters*, *45*(7), 3193–3202, doi:10.1002/2017GL076164.

Kobayashi, S., et al. (2015), The JRA-55 reanalysis: General specifications and basic characteristics, *Journal of the Meteorological Society of Japan*, *93*(1), 5–48, doi:10.2151/jmsj.2015-001.

Meinen, C. S., R. C. Perez, S. Dong, A. R. Piola, and E. Campos (2020), Observed Ocean Bottom Temperature Variability at Four Sites in the Northwestern Argentine Basin: Evidence of Decadal Deep/Abyssal Warming Amidst Hourly to Interannual Variability During 2009–2019, *Geophysical Research Letters*, *47*(18), doi:10.1029/2020GL089093.

Mertens, C., M. Rhein, M. Walter, C. W. Böning, E. Behrens, D. Kieke, R. Steinfeldt, and U. Stöber (2014), Circulation and transports in the Newfoundland Basin, western subpolar North Atlantic, *Journal of Geophysical Research: Oceans*, *119*(11), 7772–7793, doi:https://doi.org/10.1002/2014JC010019.

Mills, K. E., et al. (2013), Fisheries management in a changing climate: Lessons from the 2012 ocean heat wave in the Northwest Atlantic, *Oceanography*, *26*(2), doi:10.5670/oceanog.2013.27.

Oliver, E. C., et al. (2018), Longer and more frequent marine heatwaves over the past century, *Nature Communications*, *9*(1), 1–12, doi:10.1038/s41467-018-03732-9.

Oliver, E. C. J., J. A. Benthuysen, S. Darmaraki, M. G. Donat, A. J. Hobday, N. J. Holbrook, R. W. Schlegel, and A. S. Gupta (2020), Marine Heatwaves, *Annual Review of Marine Science*, doi:https://doi.org/10.1146/annurev-marine-032720-095144.

Reynolds, R. W., T. M. Smith, C. Liu, D. B. Chelton, K. S. Casey, and M. G. Schlax (2007), Daily high-resolution-blended analyses for sea surface temperature, *Journal of Climate*, *20*(22), 5473–5496, doi:10.1175/2007JCLI1824.1.

Richaud, B., Y. O. Kwon, T. M. Joyce, P. S. Fratantoni, and S. J. Lentz (2016), Surface and bottom temperature and salinity climatology along the continental shelf off the Canadian and U.S. East Coasts, *Continental Shelf Research*, *124*, 165–181, doi:10.1016/j.csr.2016.06.005.

Rieck, J. K., C. W. Böning, and K. Getzlaff (2019), The nature of eddy kinetic energy in the labrador sea: Different types of mesoscale eddies, their temporal variability,

and impact on deep convection, *Journal of Physical Oceanography*, *49*(8), 2075–2094, doi:10.1175/JPO-D-18-0243.1.

Rosmorduc, V., C. Maheu, Y. Faug, and A. Date (2015), For Sea Level SLA products, *Copernicus Marine Service*, *1*(March), 0–80.

Ryan, S., C. C. Ummenhofer, G. Gawarkiewicz, P. Wagner, M. Scheinert, A. Biastoch, and C. W. Böning (2020), Depth structure of Ningaloo Niño/Niña events and associated drivers, *Journal of Climate*, pp. 1–65, doi:10.1175/jcli-d-19-1020.1.

Saba, V. S., et al. (2015), Enhanced warming of the Northwest Atlantic Ocean underclimate change, *Journal of Geophysical Research: Oceans*, *120*, 1–15, doi:10.1002/2015JC011346.

Schaeffer, A., and M. Roughan (2017), Subsurface intensification of marine heatwaves off southeastern Australia: The role of stratification and local winds, *Geophysical Research Letters*, *44*(10), 5025–5033, doi:10.1002/2017GL073714.

Shapiro, L. J., and S. B. Goldenberg (1998), Atlantic sea surface temperatures and tropical cyclone formation, *Journal of Climate*, *11*(4), 578–590, doi:10.1175/1520-0442(1998)011<0578:ASSTAT>2.0.CO;2.

Short, J., T. Foster, J. Falter, G. A. Kendrick, and M. T. McCulloch (2015), Crustose coralline algal growth, calcification and mortality following a marine heatwave in Western Australia, *Continental Shelf Research*, *106*, 38–44, doi:10.1016/j.csr.2015.07.003.

Smale, D. A., et al. (2019), Marine heatwaves threaten global biodiversity and the provision of ecosystem services, *Nature Climate Change*, *9*(4), 306–312, doi:10.1038/s41558-019-0412-1.

Tsujino, H., et al. (2018), JRA-55 based surface dataset for driving ocean–sea-ice models (JRA55-do), *Ocean Modelling*, *130*(July), 79–139, doi:10.1016/j.ocemod.2018.07.002.

Wernberg, T. (2020), Marine heatwave drives collapse of kelp forests in Western Australia, *Ecosystem collapse and climate change*, *1*(2020).

Wernberg, T., D. A. Smale, F. Tuya, M. S. Thomsen, T. J. Langlois, T. De Bettignies, S. Bennett, and C. S. Rousseaux (2013), An extreme climatic event alters marine ecosystem structure in a global biodiversity hotspot, *Nature Climate Change*, *3*(1), 78–82, doi:10.1038/nclimate1627.

Wu, L., et al. (2012), Enhanced warming over the global subtropical western boundary currents, *Nature Climate Change*, *2*(3), 161–166, doi:10.1038/nclimate1353.

7. Appendix

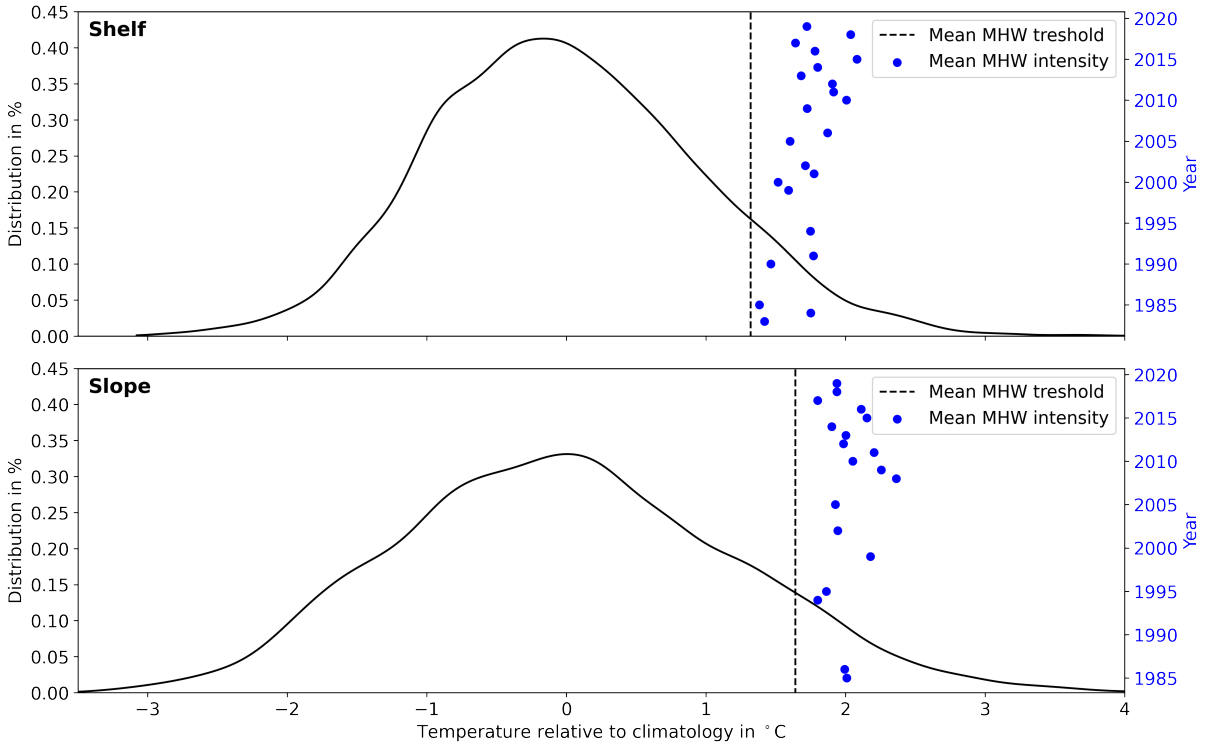

Figure A1: Probability distributions of daily sea surface temperatures relative to the climatology for shelf and slope; dashed black line indicates mean MHW threshold; dots indicate mean MHW intensity for each year in which MHWs were detected

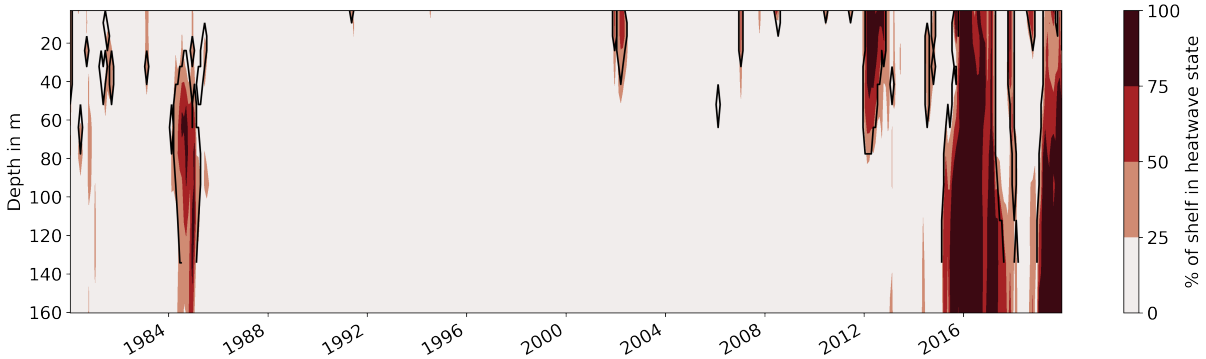

Figure A2: VIKING20X MHW detection; black contour lines show detected MHWs from the spatial mean field; colors show the spatially averaged 3D field of detected MHWs and the percentage of the shelf experiencing the MHW

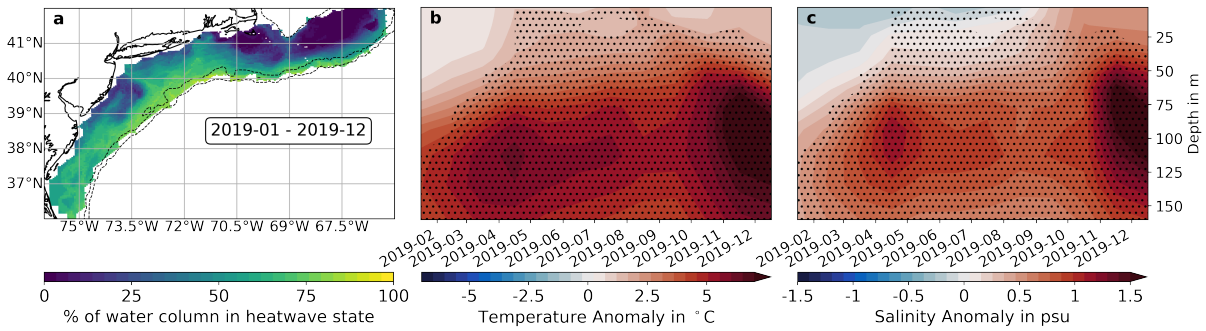

Figure A3: Distribution (a) and horizontal mean temperature (b) and salinity anomalies (c) over depth for the MHW of 2019; black contour lines in a are isobaths of 100m and 500m depth; hatching in b,c indicates MHW state (exceeding 90th percentile)

Acknowledgements

I would like to thank Svenja Ryan and Arne Biastoch for giving me this opportunity and for their great supervision. I also want to thank Caroline Ummenhofer and Torge Martin for their input during many discussions and meetings.

Eidesstattliche Erklärung

Hiermit erkläre ich, dass ich die vorliegende Arbeit selbstständig und ohne fremde Hilfe angefertigt und keine anderen als die angegebenen Quellen und Hilfsmittel verwendet habe. Die eingereichte schriftliche Fassung der Arbeit entspricht der auf dem elektronischen Speichermedium. Weiterhin versichere ich, dass diese Arbeit noch nicht als Abschlussarbeit an anderer Stelle vorgelegen hat.

Datum: 10.12.2020 Unterschrift: